DYNAMICAL PROCESSING OF GEOPHYSICAL SIGNATURES BASED ON SPOT-5 REMOTE SENSING IMAGERY

Ivan E. Villalon-Turrubiates, *Member, IEEE*

Universidad de Guadalajara, Centro Universitario de los Valles
Carretera Guadalajara-Ameca Km. 45.5, 46600 Ameca Jalisco, México, villalon@ieee.org

ABSTRACT

An intelligent post-processing computational paradigm based on the use of dynamical filtering techniques modified to enhance the quality of reconstruction of geophysical signatures based on Spot-5 imagery is proposed. As a matter of particular study, a robust algorithm is reported for the analysis of the dynamic behavior of geophysical indexes extracted from the real-world remotely sensed scenes. The simulation results verify the efficiency of the approach as required for decision support in resources management.

1. INTRODUCTION

Intelligent post-processing of the environmental monitoring data is now a mature and well developed research field, presented and detailed in many works (see for example, recent studies [1] thru [9] and the references therein). Although the existing methods offer a manifold of efficient statistical and descriptive regularization techniques to tackle with the particular environmental monitoring problems, in many application areas there still remain some unresolved theoretical and data processing problems related particularly to the extraction and analysis of the dynamical behavior of geophysical characteristics for decision support applications. In particular, the crucial data processing aspect is how to incorporate a geophysical remote sensing signatures (GRSS) extraction method with a robust dynamic analysis technique for evaluation and prediction of the behavior of the particular index monitored in environmental processes.

In this study, a robust filtering method is proposed and verified via computational simulations, which provides the possibility to track, filter and predict the dynamical behavior of the GRSS using remote sensing (RS) scenes based on Spot-5 imagery provided with the use of the recently developed Weighted Pixel Statistics (WPS) method [9]. The proposed methodology aggregates the WPS method with a dynamical filtering technique recently developed [3] via the Hydrological Dynamics method (HDM). In the simulations, the process is tested with the use of high-resolution Spot-5 imagery [10].

This study intends to show the foundations in understanding the basic theoretical and computational aspects of how to aggregate the end-user-oriented intelligent post-processing of GRSS hydrological electronic maps with the dynamic filtering paradigm (via HDM) for intelligent analysis of the dynamical behavior of the remotely monitored scenes.

The reported results of simulation study and their analysis are indicative of a usefulness of the proposed approach for monitoring the geophysical characteristics, and those could be addressed for different end-user-oriented resources management applications.

2. PROBLEM MODEL

Consider the measurement data wavefield $u(\mathbf{y})=s(\mathbf{y})+n(\mathbf{y})$ modeled as a superposition of the echo signals s and additive noise n that assumed to be available for observations and recordings within the prescribed time-space observation domain $Y \ni \mathbf{y}$. The model of observation wavefield u is specified by the linear stochastic equation of observation (EO) of operator form [1] as $u=Se+n$ ($e \in$ E; $u,n \in$ U; S:E$\rightarrow$U) in the L_2 Hilbert signal spaces E and U [1] with the metric structures induced by inner products,

$$[e_1,e_2]_{\mathrm{E}}= \int_{F\times X} e_1(f,\mathbf{x})e_2^*(f,\mathbf{x})dfd\mathbf{x}\,,$$
$$[u_1,u_2]_{\mathrm{U}}=\int_{Y} u_1(\mathbf{y})u_2^*(\mathbf{y})d\mathbf{y}\,, \qquad (1)$$

respectively, where * stands for complex conjugate. The operator model of the stochastic EO in the conventional integral form may be rewritten as [1]

$$u(\mathbf{y})= \int_{F\times X} S(\mathbf{y},\mathbf{x})e(f,\mathbf{x})dfd\mathbf{x} + n(\mathbf{y})\,,$$
$$e(f,\mathbf{x})= \int_{T} \varepsilon(t;\mathbf{x})\exp(-j2\pi ft)dt\,, \qquad (2)$$

where $\varepsilon(t;\mathbf{x})$ represents the stochastic backscattered wavefield fluctuating in time t, and the functional kernel $S(\mathbf{y},\mathbf{x})$ of the signal formation operator (SFO) S in (2) is specified by the particular employed RS signal wavefield formation model [2]. The phasor $e(f,\mathbf{x})$ in (2) represents the backscattered wavefield $e(f)$ over the frequency-space observation domain $F\times P\times\Theta$ [1], in the slant range $\rho\in P$ and azimuth angle $\theta\in\Theta$ domains, $\mathbf{x}=(\rho,\theta)^{\mathrm{T}}$, $\mathbf{X}=P\times\Theta$, respectively. The RS imaging problem is to find an estimate $\hat{B}(\mathbf{x})$ of the power spatial spectrum pattern (SSP) $B(\mathbf{x})$ ([3]

and [4]) in the $X\ni\mathbf{x}$ environment via processing whatever values of measurements of the data wavefield $u(\mathbf{y})$, $\mathbf{y}\in Y$ are available. Following the RS methodology [1], any particular GRSS of interest is to be extracted from the reconstructed RS image $\hat{B}(\mathbf{x})$ applying the so-called signature extraction operator Λ [5]. The particular GRSS is mapped applying Λ to the reconstructed image, i.e.

$$\hat{\Lambda}(\mathbf{x}) = \Lambda(\hat{B}(\mathbf{x})) \,. \quad (3)$$

Taking into account the GRSS extraction model (3), the signature reconstruction problem is formulated as follows: to map the reconstructed particular GRSS of interest $\hat{\Lambda}(\mathbf{x}) = \Lambda(\hat{B}(\mathbf{x}))$ over the observation scene $X\ni\mathbf{x}$ via post-processing (4) whatever values of the reconstructed scene image $\hat{B}(\mathbf{x})$, $\mathbf{x}\in X$ are available.

3. IMAGE SEGMENTATION AND CLASSIFICATION

The development of a novel tool for supervised segmentation and classification of GRSS from multispectral remote sensing (MRS) imagery is based on the analysis of pixel statistics, and is referred to as the weighted pixel statistics (WPS) method, which was recently developed [9].

The WPS classificatory rule is computationally simple and provides classification accuracy comparable to other more computationally intensive algorithms [9]. It is characterized by the mean and variance values of the GRSS signatures (classes) and the Euclidean distances based on the Pythagorean Theorem. An important aspect of this method is that it is applied to the MRS imagery.

The training data for class segmentation requires the number of GRSS to be classified (c); the means matrix **M** ($c\times c$ size) that contains the mean values μ_{cc}: ($0 \le \mu_{cc} \le 255$, gray-level) of the GRSS classes for each RGB bands; and the variances matrix **V** ($c\times c$ size) that contains the variances of the GRSS classes for each RGB bands. The matrix **M** and **V** represents the weights of the classification process.

Next, the image is separated in the spectral bands (R, G and B) and each (i, j)-*th* pixel is statistically analyzed calculating the means and variances from a neighborhood set of *5x5* pixels for each RGB band, respectively.

To compute the output of the classifier, the distances between the pixel statistics and the training data is calculated using Euclidean distances based on the Pythagorean Theorem for means and variances, respectively.

The decision rule used by the WPS method is based on the minimum distances gained between the weighted training data and the pixel statistics. The WPS techniques provide a high level of GRSS segmentation and classification.

For this particular study, covered water, humid and dry zones are analyzed as particular GRSS of interest.

4. DYNAMICAL HDM COMPUTING

4.1 GRSS Lineal Dynamic Model

The crucial issue in application of the modern dynamic filter theory to the problem of reconstruction of the desired GRSS in time is related to modeling of the RS as a random field (spatial map developing in evolution time t) that satisfies some dynamical state equation.

Following the typical linear assumptions for the development of the GRSS in time [8] its dynamical model can be represented in a vectorized space-time form defined by a stochastic differential state equation of the first order

$$\frac{d\mathbf{z}(t)}{dt} = \mathbf{F}\mathbf{z}(t) + \mathbf{G}\boldsymbol{\xi}(t)\,, \quad \boldsymbol{\Lambda}(t) = \mathbf{C}\mathbf{z}(t) \quad (4)$$

where $\mathbf{z}(t)$ is the so-called model state vector, **C** defines a linear operator that introduces the relationship between the GRSS and the state vector $\mathbf{z}(t)$, and $\boldsymbol{\xi}(t)$ represents the white model generation noise vector characterized by the statistics $\langle\boldsymbol{\xi}(t)\rangle = \mathbf{0}$ and $\langle\boldsymbol{\xi}(t)\boldsymbol{\xi}^T(t')\rangle = \mathbf{P}_{\xi}(t)\delta(t-t')$ [8]. Here, $\mathbf{P}_{\xi}(t)$ is referred to as state model disperse matrix [8] that characterizes the dynamics of the state variances developing in a continuous time t ($t_0 \to t$) starting from the initial instant t_0.

The dynamic model equation that states the relationship between the time-dependent SSP (actual scene image) $\mathbf{B}(t)$ and the desired GRSS map $\boldsymbol{\Lambda}(t)$ represented as [8]

$$\hat{\mathbf{B}}(t) = \mathbf{H}(t)\mathbf{z}(t) + \mathbf{v}(t)\,, \quad \mathbf{H}(t) = \mathbf{L}\mathbf{C}(t), \quad (5)$$

where **L** is the linear approximation (i.e. first order matrix-form approximation [3]) to the inverse of the GRSS operator $\Lambda(\hat{B}(\mathbf{r}))$. The stochastic differential model (4) and (5) allows the application of dynamical filter theory [3], [4] to reconstruct the desired GRSS in evolution time incorporating the a priori model of dynamical information about the GRSS.

The aim of the dynamic filtration is to find an optimal estimate of the desired GRSS $\hat{\boldsymbol{\Lambda}}(t) = \mathbf{C}\hat{\mathbf{z}}(t)$ developing in time t ($t_0 \to t$) via processing the reconstructed image vector $\hat{\mathbf{B}}(t)$ and taking into considerations the a priori dynamic model of the desired GRSS specified through the state equation (4). In other words, the design of an optimal dynamic filter that, when applied to the reconstructed image $\hat{\mathbf{B}}(t)$, provides the optimal estimation of the desired GRSS map $\hat{\boldsymbol{\Lambda}}(t)$, in which the state vector estimate $\hat{\mathbf{z}}(t)$ satisfies the a priori dynamic behavior modeled by the stochastic dynamic state equation (4). The canonical discrete time solution to (4) in state variables [9] is described as follows,

$$\mathbf{z}(i+1) = \boldsymbol{\Phi}(i)\mathbf{z}(i) + \boldsymbol{\Gamma}(i)\mathbf{x}(i)\,, \quad \boldsymbol{\Lambda}(i) = \mathbf{C}(i)\mathbf{z}(i)\,, \quad (6)$$

where $\boldsymbol{\Phi}(i) = \mathbf{F}(t_i)\Delta t + \mathbf{I}$, $\boldsymbol{\Gamma}(i) = \mathbf{G}(t_i)\Delta t$, and Δt represents the time sampling interval for dynamical modeling of the GRSS in discrete time. The statistical characteristics of the a priori information in discrete-time [8] are specified as

1) Generating noise: $\langle \xi(i) \rangle = \mathbf{0}$; $\left\langle \xi(i)\xi^T(j) \right\rangle = \mathbf{P}_\xi(i,j)$;

2) Data noise: $\langle \mathbf{v}(k) \rangle = \mathbf{0}$; $\left\langle \mathbf{v}(i)\mathbf{v}^T(j) \right\rangle = \mathbf{P}_\mathbf{v}(i,j)$;

3) State vector: $\langle \mathbf{z}(0) \rangle = \mathbf{m}_z(0)$; $\left\langle \mathbf{z}(0)\mathbf{z}^T(0) \right\rangle = \mathbf{P}_\mathbf{z}(0)$.

The **0** argument implies the initial state for initial time instant (i=0). For such model conventions, the disperse matrix $\mathbf{P}_z(0)$ satisfies the following disperse dynamic equation [8]

$$\mathbf{P}_\mathbf{z}(i+1) = \mathbf{\Phi}(i)\mathbf{P}_\mathbf{z}(i)\mathbf{\Phi}^T(i) + \mathbf{\Gamma}(i)\mathbf{P}_\xi(i)\mathbf{\Gamma}^T(i)\,. \tag{7}$$

4.2 Dynamic GRSS Reconstruction

The problem is to design an optimal decision procedure that, when applied to all reconstructed images $\{\hat{\mathbf{B}}(i)\}$ in discrete time i ($i_0 \rightarrow i$), provides an optimal solution to the desired GRSS represented via the estimate of the state vector state vector $\mathbf{z}(i)$ subject to the numerical dynamic model (6). To proceed with the derivation of such a filter, the state equation (4) in discrete time i ($i_0 \rightarrow i$) is represented as

$$\mathbf{z}(i+1) = \mathbf{\Phi}(i)\mathbf{z}(i) + \mathbf{\Gamma}(i)\xi(i)\,, \tag{8}$$

according to this dynamical model, the anticipated mean value for the state vector can be expressed as

$$\mathbf{m}_\mathbf{z}(i+1) = \left\langle \mathbf{z}(i+1) \right\rangle = \left\langle \mathbf{z}(i+1) \middle| \hat{\mathbf{z}}(i) \right\rangle, \tag{9}$$

where the $\mathbf{m}_\mathbf{z}(i+1)$ is considered as the a priori conditional mean-value of the state vector for the (i+1) estimation step

$$\mathbf{m}_\mathbf{z}(i+1) = \mathbf{\Phi}\left\langle \mathbf{z}(i) \middle| \hat{\mathbf{B}}(0), \hat{\mathbf{B}}(1), ..., \hat{\mathbf{B}}(i) \right\rangle + \mathbf{\Gamma}\left\langle \xi(i) \right\rangle = \mathbf{\Phi}\hat{\mathbf{z}}(i) \tag{10}$$

and the prognosis of the mean-value becomes $\mathbf{m}_\mathbf{z}(i+1) = \mathbf{\Phi}\hat{\mathbf{z}}(i)$. From (8) thru (10) is possible to deduce that given the fact that the particular reconstructed image $\hat{\mathbf{B}}(i)$ is treated at discrete time i, it makes the previous reconstructions $\{\hat{\mathbf{B}}(0), \hat{\mathbf{B}}(1), ..., \hat{\mathbf{B}}(i-1)\}$ irrelevant; hence the optimal filtering strategy is reduced to the dynamical one-step predictor. Thus, the dynamical estimation strategy is modified to one-step optimal prediction procedure

$$\hat{\mathbf{z}}(i+1) = \left\langle \mathbf{z}(i+1) \middle| \hat{\mathbf{z}}(i); \hat{\mathbf{B}}(i+1) \right\rangle = \left\langle \mathbf{z}(i+1) \middle| \hat{\mathbf{B}}(i+1); \mathbf{m}_\mathbf{z}(i+1) \right\rangle \tag{11}$$

hence, for the evolution (i+1)st discrete-time prediction-estimation step, the dynamical GRSS estimate (5) becomes

$$\hat{\mathbf{B}}(i+1) = \mathbf{H}(i+1)\mathbf{z}(i+1) + \mathbf{v}(i+1) \tag{12}$$

with the a priori predicted mean (9) for the desired state vector. Applying the Wiener minimum risk strategy [8] to solve (12) with respect to the state vector $\mathbf{z}(t)$ and taking into account the a priori information, the dynamic solution for the RSS state vector becomes

$$\hat{\mathbf{z}}(i+1) = \mathbf{m}_\mathbf{z}(i+1) + \mathbf{\Sigma}(i+1)\left[\hat{\mathbf{B}}(i+1) - \mathbf{H}(i+1)\mathbf{m}_\mathbf{z}(i+1)\right] \tag{13}$$

where the desired dynamic filter operator $\mathbf{\Sigma}(i+1)$ is

$$\mathbf{\Sigma}(i+1) = \mathbf{K}_\mathbf{\Sigma}(i+1)\mathbf{H}^T(i+1)\mathbf{P}_\mathbf{v}^{-1}(i+1)\,,$$
$$\mathbf{K}_\mathbf{\Sigma}(i+1) = \left[\mathbf{\Psi}_\mathbf{\Sigma}(i+1) + \mathbf{P}_\mathbf{z}^{-1}(i+1)\right]^{-1}, \tag{14}$$
$$\mathbf{\Psi}_\mathbf{\Sigma}(i+1) = \mathbf{H}^T(i+1)\mathbf{P}_\mathbf{v}^{-1}(i+1)\mathbf{H}(i+1)\,.$$

Using the derived filter equations (13) and (14) and the initial GRSS state model given by (6), the optimal filtering procedure for dynamic reconstruction becomes

$$\hat{\mathbf{\Lambda}}(i+1) = \mathbf{\Phi}(i)\hat{\mathbf{z}}(i) + \mathbf{\Sigma}(i+1)\left[\hat{\mathbf{B}}(i+1) - \mathbf{H}(i+1)\mathbf{\Phi}(i)\hat{\mathbf{z}}(i)\right] \tag{15}$$

with the initial condition $\hat{\mathbf{\Lambda}}(0) = \Lambda\{\hat{\mathbf{B}}(0)\}$. The crucial issue to note here is related to model uncertainties regarding the particular employed dynamical GRSS model (6), hence the model mismatch uncertainties regarding the overall dynamically reconstructed GRSS.

5. SIMULATIONS

In the reported here simulation results, a hydrological GRSS electronic map is extracted from the Spot-5 MRS imagery (high-resolution) using the WPS methods. Three level of GRSS are selected for this particular simulation process, moreover, unclassified zones must be also considered (2-bit classification) as

– GRSS relative to the wet zones of the MRS image.
– GRSS relative to the humid zones of the MRS image.
– GRSS relative to the dry zones of the MRS image.
– Unclassified zones of the GRSS map.

Figure 1 shows the MRS *1024x1024*-pixels RGB image in TIFF format borrowed from Spot-5 imagery [10] corresponding to the Banderas Bay in the city of Puerto Vallarta, Mexico.

Figure 2 shows the hydrological GRSS map obtained applying the WPS method for the adopted ordered weight vector. The WPS method employs all three RGB bands; therefore, using the statistical pixel-based information the hydrological GRSS map obtained shows a high-accurate classification without unclassified zones.

Figure 3 shows the results of the dynamical analysis obtained after the processing of 40 hydrological GRSS maps (images not shown) in discrete-time with the application of the derived HDM algorithm (15). These simulations present the evolution in time of the physical characteristics specified via the hydrological GRSS maps.

6. CONCLUDING REMARKS

In this paper, the dynamical approach for solving the nonlinear inverse problems of high-resolution dynamical reconstruction of the hydrological GRSS of the environmental scenes is presented via processing the finite-dimensional space-time measurements of the available sensor data. The dynamical GRSS post-processing scheme reveals some possible approach toward a new dynamic computational paradigm for high-resolution fused numerical reconstruction and filtration of different GRSS maps in discrete time. The presented study establishes the foundation to assist in understanding the basic theoretical and computational aspects of RS image enhancement, extraction of physical scene characteristics and their dynamical post-processing.

Figure 1. Original high resolution MRS image.

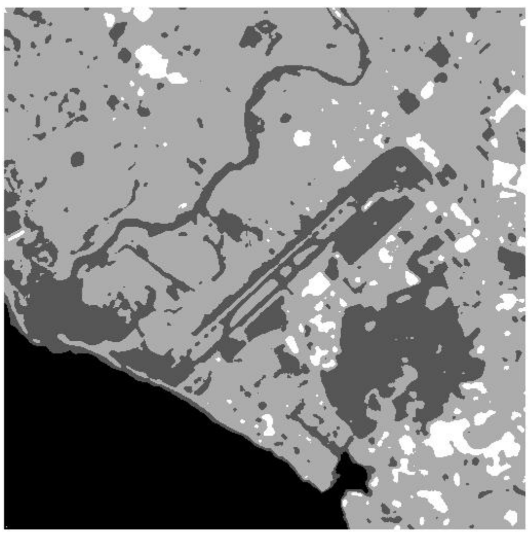

Figure 2. GRSS hydrological map extracted with WPS.

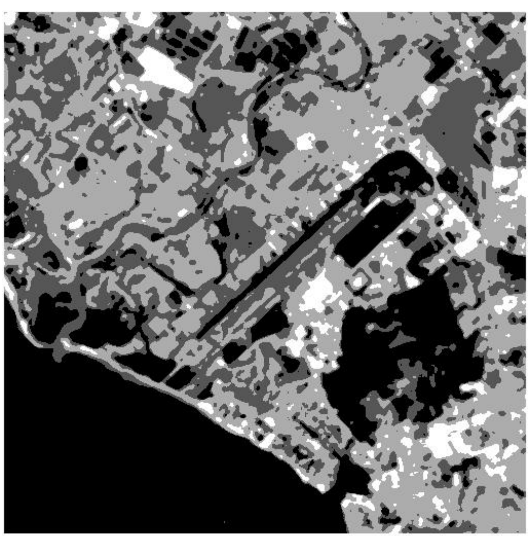

Figure 3. Dynamic GRSS hydrological map obtained with HDM.

The reported results of simulation study are indicative of a usefulness of the proposed approach for monitoring the physical environmental characteristics, and those could be addressed for different end-user-oriented environmental resource management applications.

7. ACKNOWLEDGMENT

The author would like to thank the "Programa de Mejoramiento del Profesorado PROMEP" of the Public Education Secretary (SEP) of Mexico and the University of Guadalajara for the resources provided for this research.

8. REFERENCES

[1] Y.V. Shkvarko, "Estimation of wavefield power distribution in the remotely sensed environment: bayesian maximum entropy approach", *IEEE Transactions on Signal Processing*, vol. 50, 2002, pp. 2333-2346.

[2] B.R. Mahafza, *Radar Systems Analysis and Design Using MATLAB*, CRC Press, USA, 2000.

[3] Y.V. Shkvarko and I.E. Villalon-Turrubiates, "Remote sensing imagery and signature fields reconstruction via aggregation of robust regularization with neural computing", in *Advanced Concepts for Intelligent Vision Systems*, J. Blanc-Talon, W. Philips, D. Popescu, P. Scheunders, Eds. Berlin: Springer-Verlag, 2007, pp. 235-246.

[4] Y.V. Shkvarko and I.E. Villalon-Turrubiates, "Computational enhancement of large scale environmental imagery: aggregation of robust numerical regularization, neural computing and digital dynamic filtering", in *Journal of Computational Science and Engineering*, vol. 3, Inderscience Eds. 2007, pp. 219-231.

[5] I.E. Villalon-Turrubiates and Y.V. Shkvarko, "Dynamical post-processing of environmental electronic maps extracted from large scale remote sensing imagery", *IEEE International Geoscience and Remote Sensing Symposium*, Barcelona: IEEE Press, 2007, pp. 1485-1488.

[6] S.W. Perry, S.W, H.S. Wong and L. Guan, *Adaptive Image Processing: A Computational Intelligence Perspective*, CRC Press, USA, 2002.

[7] J.R. Jensen, *Introductory Digital Image Processing: A Remote Sensing Perspective*, 3rd ed., Pearson, 2005.

[8] S.E. Falkovich, V.I. Ponomaryov and Y.V. Shkvarko, *Optimal Reception of Space-Time Signals in Channels with Scattering*, Radio I Sviaz, Russia, 1989.

[9] I.E. Villalon-Turrubiates, "Weighted pixel statistics for multispectral image classification of remote sensing signatures: performance study", *Proceedings of the 5th IEEE International Conference of Electrical engineering, Computing Science and Automatic Control*, in press.

[10] Spot Image, in: http://www.spotimage.com, Spot Image S.A., 2008.